Theoretical Study on the Potential Energy Surface of the $^1CH_2+N_2O$ Reaction

Jian-jun Liu, Ji-kang Feng,* Yi-hong Ding, Ai-min Ren, Su-fan Wang, and Chia-chung Sun

State Key Laboratory of Theoretical and Computational Chemistry, Jilin University, Changchun, Jilin 130023, P. R. China

Fan-ao Kong

Laboratory of Molecular Reaction Dynamics, Institute of Chemistry, Academia Sinica, Beijing 100085, P. R. China

Received: April 20, 2000; In Final Form: August 17, 2000

The complex potential energy surface for the reaction of singlet methylene ($^1CH_2$) with nitrous oxide (N_2O) has been investigated in detail using B3LYP/6-31G(d,p) and single-point QCISD(T)/6-311G(d,p) methods. The association of $^1CH_2$ with N_2O was found to be a barrierless process forming an energy-rich adduct CH_2-NNO (a_1). Our calculations show that the products $P_1(N_2+H_2CO)$ and $P_{13}(NO+HCN+H)$ are the major products for the title reaction. The other products, including CO and H_2, are minor products. The product $P_1(N_2+H_2$-CO) can be obtained through R→a_1→a_2→b→ $P_1(N_2+H_2CO)$ (r1), whereas the product $P_{13}(NO+HCN+H)$ can be obtained through two competitive channels R→a_1→$P_4(HNO+HCN)$→$P_{13}(NO+HCN+H)$ (r8) and R→a_1→a_2 →$P_5(NO+H_2CN)$→$P_{13}(NO+HCN+H)$ (r12). At high temperatures, the direct abstraction channel leading to product N_2+H_2CO may become feasible. Our work can assist experiments to identify the products of the $^1CH_2+N_2O$ reaction.

1. Introduction

The reaction of nitrous oxide (N_2O) continues to attract the attention of both experimental and theoretical chemists due to its role as an important species in combustion and atmospheric processes.[1] Being the simplest carbene, methylene (CH_2) is amenable to theoretical studies and is thus a prototype for this important class of organic intermediates.[2] Furthermore, CH_2 plays an important role in combustion and flames.[3,4] The reaction of CH_2 with N_2O is of potential relevance to the "reburn" technology, which is an efficient method for reducing N_2O emissions in many combustion processes.

Bell et al.[5] studied the reaction of singlet $^1CH_2$ with the N_2O molecule by gas chromatography and mass spectroscopy. However, they found no evidence showing that $^1CH_2$ reacted with N_2O. Using the pulsed laser, photolysis generation−LIF detection method for $^1CH_2$, Koch et al.[7] determined that the experimental rate constant of the reaction $^1CH_2+N_2O$ is $3.8 \pm 0.4 \times 10^{13}$cm^2/mol·s at room temperature. The rate constant was found to be pressure independent at room temperature. According to the thermochemical data, Koch et al.[7] proposed the reaction channels, but the exact products were not measured. Recently, Su et al.[6] studied the triplet $^3CH_2$ reaction with N_2O. They observed the IR emissions from the nascent vibrationally excited products CO(v), NO(v), HCN(v), and HCN or N_2H by TR−FTIR spectroscopy. The dynamical investigations of the $^1CH_2+N_2O$ reaction are in progress in their laboratory. Considering that measurements of the product distribution of the $^1CH_2+N_2O$ reaction have not been reported yet, a theoretical characterization of the potential energy surface of the $^1CH_2+N_2O$ reaction is very desirable. Such a theoretical study would resolve the question of which products are indeed energetically accessible by the thermal reactants $^1CH_2+N_2O$ so as to assist in experimental identification.

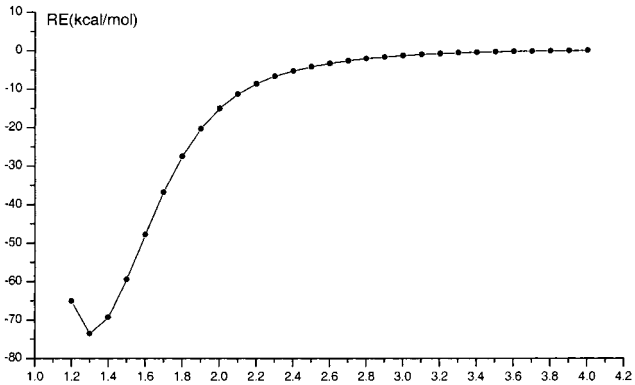

Figure 1. Relaxed potential energy curve for the formative process of the adduct (a_1) at the B3LYP/6-31G(d,p) level. The distance between the C atom and the end N atom was varied from 1.2 to 4.0 Å with an interval of 0.1 Å. We retained the C_s symmetry in the adduct (a_1). Other geometric parameters were optimized for each value of the C−N distance.

The large and pressure-independent value of the rate constant at room temperature suggests a zero or very low entrance barrier. Furthermore, it leads us to conclude that the $^1CH_2+N_2O$ reaction may proceed via an association−elimination mechanism. Since the reaction involves the initial association of $^1CH_2$ and N_2O, the products of the reaction must be related to [C, H_2, N_2, O] isomers. Therefore, it is essential to obtain knowledge about various isomers, transition states, and their energetics in order to gain a better understanding of the reaction mechanism.

To our knowledge, a complete potential energy surface of the $^1CH_2+N_2O$ reaction has not yet been reported. As a first step toward the understanding of the $^1CH_2+N_2O$ reaction kinetics, we have explored the potential energy surface using density functional theory (B3LYP) and quadratic configuration interaction (QCISD(T)) method. Our primary aim in this

10.1021/jp001524o CCC: $20.00
Published on Web 05/22/2001

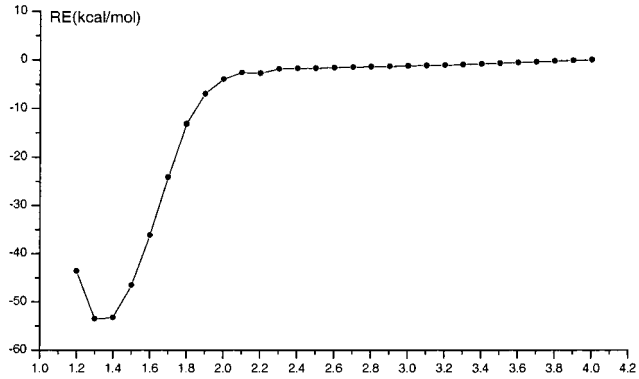

Figure 2. Relaxed potential energy curve for the formative process for the adduct (j) at the B3LYP/6-31G(d,p) level. The distance between the C atom and the center of the N−N bond was varied from 1.2 to 4.0 Å with an interval of 0.1 Å. We retained the C_s symmetry in the adduct (j). It should be particularly pointed out that we made them approach along the perpendicular bisector of the N−N bond. Other geometric parameters were optimized for each distance between the C atom and the center of the N−N bond.

investigation is to identify the product distribution and the exact channels for each of the products and thereby to gain insight into the reaction kinetics.

2. Computational Methods

All calculations are performed with the GAUSSIAN98 program. Geometries of reactants, intermediates, and products are optimized, and transition states are located using Schlegel's algorithm[8] at the B3LYP/6-31G(d,p) theory level.[9,10] The nature of all critical points is further characterized, and zero-point vibrational energies (ZPVE) are evaluated by analytical B3LYP/6-31G(d,p) computations of harmonic frequencies. All computed reaction products and intermediates have real frequencies, whereas every transition state structure has only one imaginary frequency. To confirm that the transition state connects designated intermediates, we also perform intrinsic reaction coordinate (IRC) calculations using the Gonzalez and Schlegel method[11,12] at the B3LYP/6-31G(d,p) theory level. In addition, single-point energies are calculated with the quadratic configuration interaction method with single and double excitation and perturbative corrections for triple excitations (QCISD(T))[13,14] at the optimized B3LYP/6-31G(d,p) geometries. Unless otherwise specified, the QCISD(T) single-point energies are used in the following discussions.

3. Results and Discussions

The relaxed potential energy curves for the formation of adducts (a_1) and (j) are shown in Figures 1 and 2, respectively. To clarify the reaction mechanism, the potential energy surface profiles for all reaction channels are shown in Figures 3−6 according to different primary dissociation products. The product channels related to H_2CO and HCOH(cis, trans) are shown in Figure 3, those related to NO and HCN in Figure 4, those related to H_2N_2 and HN_2H(cis, trans) in Figure 5, and those related to $CO+N_2+H_2$ and N_2H+HCO in Figure 6. Tables 1−3 display the zero-point energies, total energies, and relative energies of all the stationary points. The relative energies with reference to the reactants include zero-point vibrational energies. Equilibrium points in these profiles are labeled with lowercase letters from a to l so as to facilitate discussion. Some site isomers are labeled with the same lowercase letter and also with a number subscript, viz., a_1 a_2, e_1 e_2 e_3 e_4, f_1 f_2, h_1 h_2, and l_1 l_2. The transition structures are defined by TS*xy* where *x* and *y* are the two connected equilibrium structures. Two reactants are labeled with R, and all products with P and a number subscript, from P_1 to P_{18}. All optimized geometries of reactants and products are shown in Figure 7, the optimized geometries of isomers in

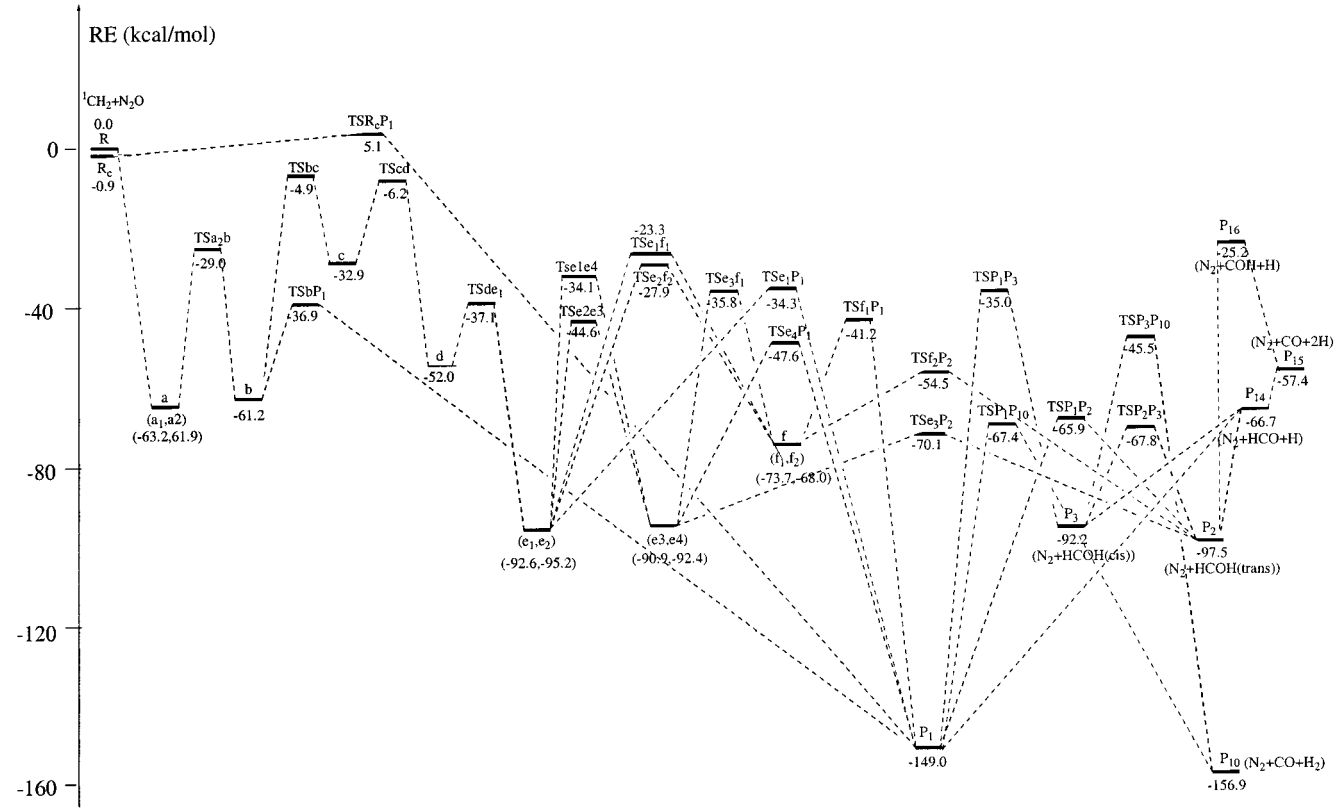

Figure 3. Schematic profile of the potential energy surface (kcal/mol) related to primary dissociation products H_2CO and HCOH (cis, trans) at the QCISD(T)/6-311G(d,p)//B3LYP/6-31G(d,p)+ZPE level for the $^1CH_2+N_2O$ reaction.

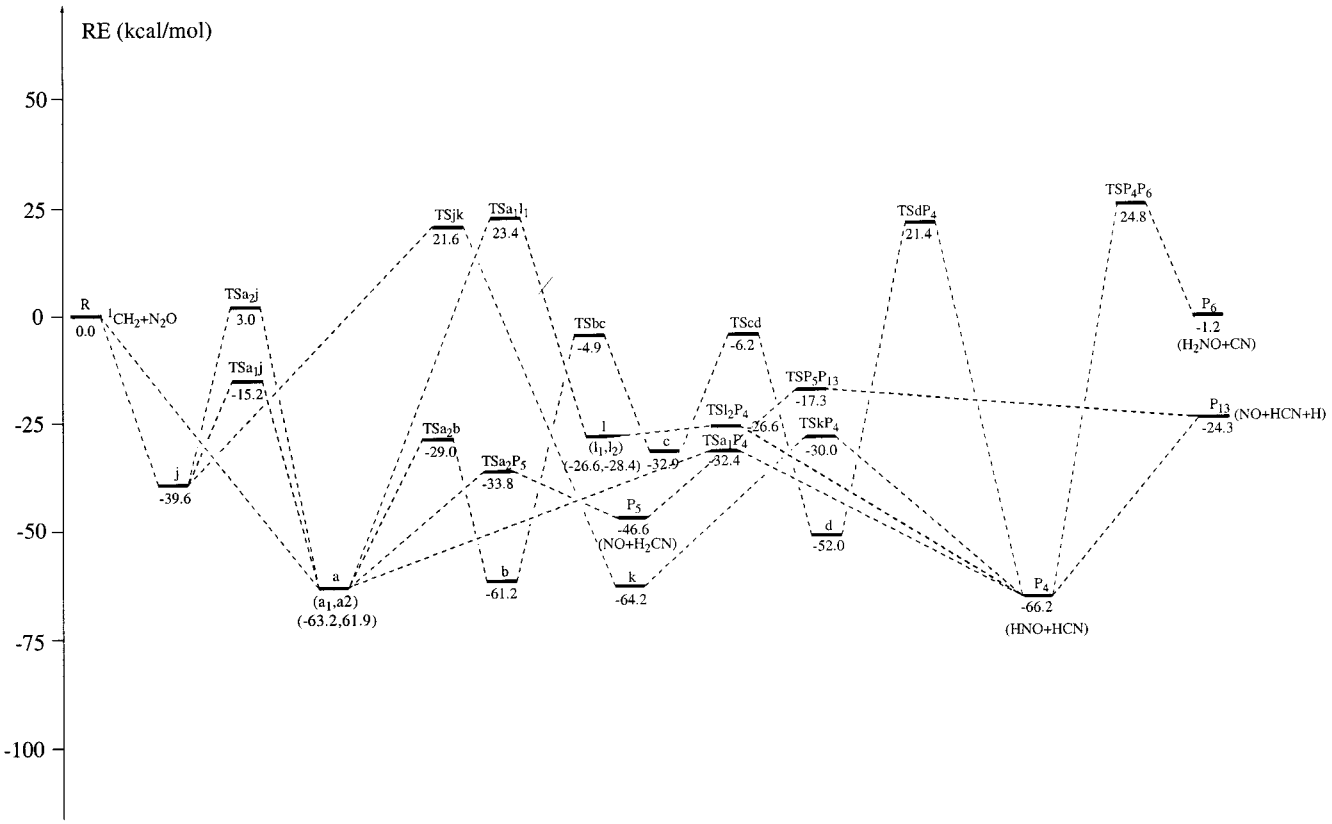

Figure 4. Schematic profile of the potential energy surface (kcal/mol) related to primary dissociation products NO and HCN at the QCISD(T)/6-311G(d,p)//B3LYP/6-31G(d,p)+ZPE level for the $^1CH_2+N_2O$ reaction.

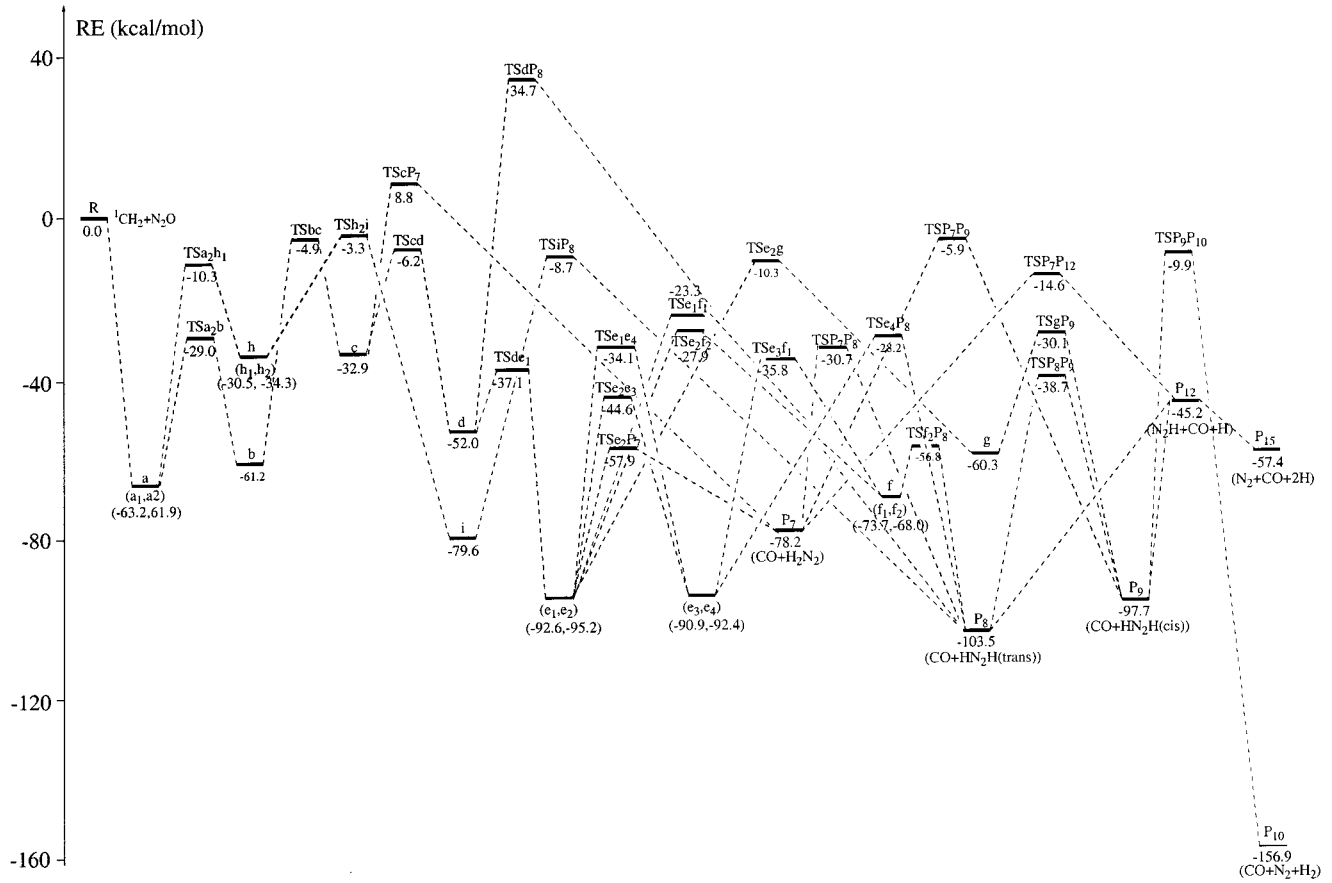

Figure 5. Schematic profile of the potential energy surface (kcal/mol) related to primary dissociation products H_2N_2 and HN_2H (cis,trans) at the QCISD(T)/6-311G(d,p)//B3LYP/6-31G(d,p)+ZPE level for the $^1CH_2+N_2O$ reaction.

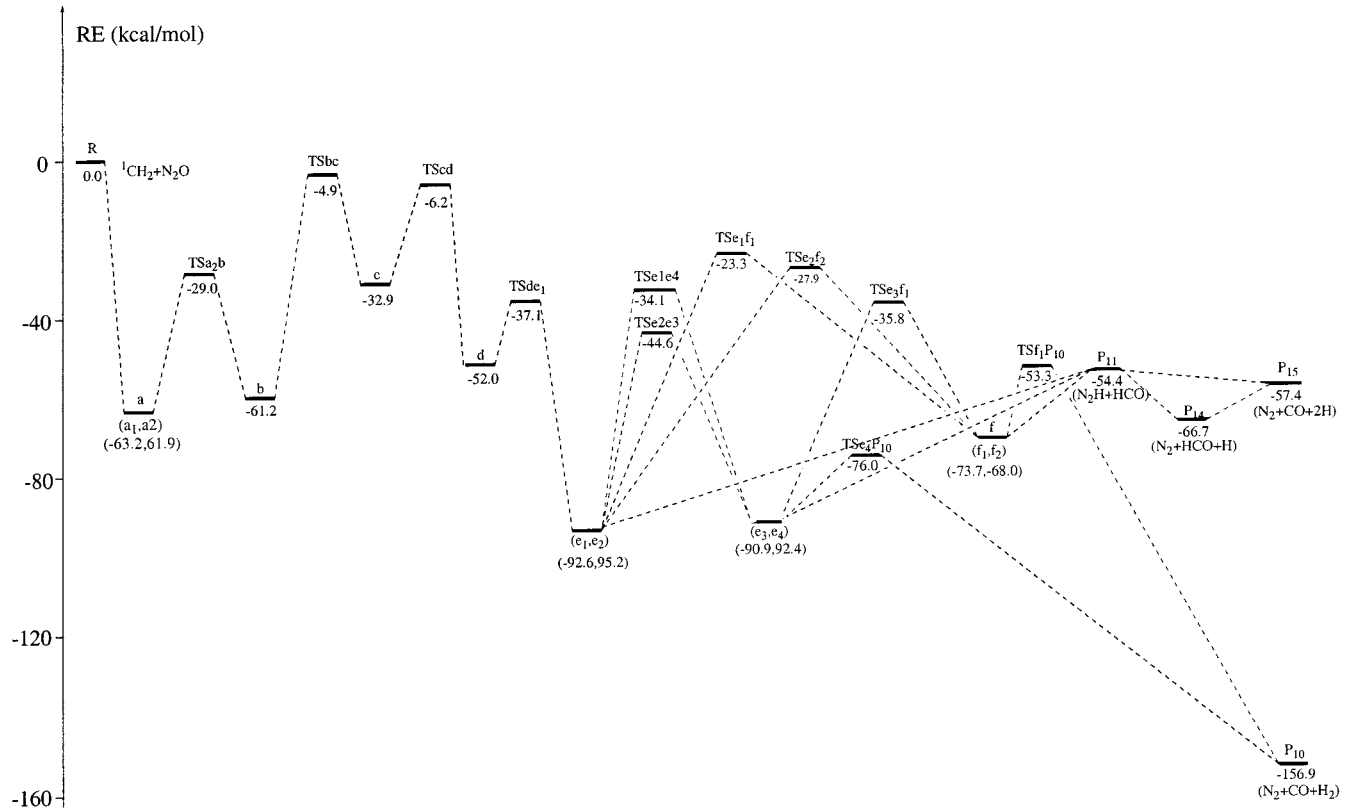

Figure 6. Schematic profile of the potential energy surface (kcal/mol) related to primary dissociation products CO+N_2+H_2 and N_2H+HCO at the QCISD(T)/6-311G(d,p)//B3LYP/6-31G(d,p)+ZPE level for the $^1CH_2$+N_2O reaction.

Figure 8, the geometries of the transition states of isomerizations in Figure 9, the geometries of the transition states of dissociation to products in Figure 10, and the geometries of the transition states of secondary dissociation in Figure 11.

3.1. Initial Association of $^1CH_2$ and N_2O. According to the studies of Harcourt et al.,[15] N_2O not only involves the N≡N triple bond but also has singlet diradical character for the terminal N atom. Hence, the paired p electrons of the C atom may attack the linear N_2O molecule in either a head-on or side-on manner. Accordingly, we focus on two entrance channels, i.e., addition to the terminal N atom and [2+1] cycloaddition to the N≡N triple bond.

The head-on attack of the C atom of $^1CH_2$ at the terminal N atom of N_2O leads to adduct CH_2N_2O (a_1). As this process involves double bond formation between diradical and lone pair electrons, a high barrier may be faced. However, all of our attempts to locate such an addition transition state were proved to be futile at the B3LYP/6-31G(d,p) level. To confirm the nonbarrier of this process, we performed point-wise calculations at the B3LYP/6-31G(d,p) level as a function of the distance between the C atom and the end N atom. The C_s symmetry of the adduct (a_1) is retained. As shown in Figure 1, the adduct (a_1) is formed as the end N atom and C atom approach each other to interact on an attractive potential energy surface. It is obvious that this addition process is a barrierless association. It can provide enough energy to make the adduct (a_1) highly activated so that further isomerization or dissociation reactions can be promoted. The association is expected to be fast and to play a significant role in the reaction kinetics.

It is well-known that singlet carbenes readily take addition reaction with double bond or triple bond, even without any activation energy. Similar to the situation of adduct (a_1), we cannot locate the transition state for the [2+1] cycloaddition between the C atom of $^1CH_2$ and the N≡N bond of N_2O to form the cyclic isomer (j) that lies 39.2 kcal/mol below the reactants. So the cycloaddition process is also characterized by calculating optimized geometries for several distances between the C atom and the center of the N−N bond. As we can see in Figure 2, [2+1] cycloaddition of the C atom to the N≡N bond is still barrierless. It should be particularly pointed out that we made them approach along the perpendicular bisector of the N−N bond. Without this constraint, $^1CH_2$ does not approach the N−N bond, but asymmetrically approaches O atom or the end N atom. This indicates that the [2+1] cycloaddition leading to isomer (j) is not the lowest energy path and may be an unfavorable reaction channel. Thus, we conclude that the three-membered ring isomer (j) may have a small or negligible role in the kinetics of the title reaction.

There are two transition states TSa_1j and TSa_2j for the interconversion between the initial adducts (a) and (j). TSa_1j is 15.2 kcal/mol below the reactants, whereas TSa_2j is 3.0 kcal/mol above the reactants. Clearly, once (j) is formed from the reactants, its conversion to (a_1) is possible via TSa_1j.

3.2. Isomerization Channels. We sum up the isomerization channels starting from the initial adducts as follows:

$$a_1 \rightarrow a_2 \rightarrow b \rightarrow c \rightarrow d \rightarrow e(e_1\ e_2\ e_3\ e_4) \rightarrow f(f_1\ f_2),\ e_2 \rightarrow g \quad \text{(i1)}$$

$$a_1 \rightarrow a_2 \rightarrow h_1 \rightarrow h_2 \rightarrow i \quad \text{(i2)}$$

$$a_1 \rightarrow l_1 \rightarrow l_2 \quad \text{(i3)}$$

$$j \rightarrow k \quad \text{(i4)}$$

At first, let us discuss the isomerization channels mentioned above. In the next section, we will continue to discuss dissociation channels from these isomers or reactants to products.

TABLE 1: Zero-Point Vibration Energies (in hartree), Total Energies (TE) (in hartree), and Relative Energies (RE) (in kcal/mol) of Reactants, Intermediates, Transition States, and Products at the B3LYP/6-31G(d,p) and QCISD(T)/6-311G(d,p)// B3LYP/6-31G(d,p) Levels

	B3LYP/6-31G(d,p)			QCISD(T)/6-311G(d,p)// B3LYP/6-31G(d,p)	
species	ZPVE	TE	RE	TE	RE
		Reactants and Products			
$R(^1CH_2+N_2O)$	0.026349	−223.792026	0.0	−223.328862	0.0
R_C	0.032461	−223.803206	−3.2	−223.336444	−0.9
$P_1(N_2+H_2CO)$	0.032324	−224.027328	−143.9	−223.572296	−149.0
$P_2(N_2+HCOH(trans))$	0.032169	−223.939910	−89.2	−223.490021	−97.5
$P_3(N_2+HCOH(cis))$	0.031270	−223.932145	−84.8	−223.480729	−92.2
$P_4(HNO+HCN)$	0.030303	−223.889526	−63.4	−223.438273	−66.2
$P_5(H_2NO+CN)$	0.031618	−223.801081	−2.4	−223.336100	−1.2
$P_6(NO+H_2CN)$	0.029818	−223.873579	−49.0	−223.406671	−46.6
$P_7(CO+H_2N_2)$	0.031605	−223.916865	−75.1	−223.458711	−78.2
$P_8(CO+HN_2H(trans))$	0.033304	−223.952464	−96.3	−223.500702	−103.5
$P_9(CO+HN_2H(cis))$	0.032586	−223.943311	−91.0	−223.490813	−97.7
$P_{10}(N_2+CO+H_2)$	0.020804	−224.012123	−141.6	−223.573389	−156.9
$P_{11}(N_2H+HCO)$	0.026292	−223.884555	−58.1	−223.415527	−54.4
$P_{12}(N_2H+CO+H)$	0.018284	−223.842452	−36.7	−223.392762	−45.2
$P_{13}(NO+HCN+H)$	0.021005	−223.806345	−17.6	−223.362271	−24.3
$P_{14}(N_2+HCO+H)$	0.018639	−223.876233	−57.7	−223.427434	−66.7
$P_{15}(N_2+CO+2H)$	0.010631	−223.834029	−36.3	−223.404669	−57.4
$P_{16}(N_2+COH+H)$	0.018740	−223.808582	−15.2	−223.361426	−25.2
$P_{17}(HNO+CN+H)$	0.018756	−223.682698	63.8	−223.236167	53.4
$P_{18}(NO+CN+2H)$	0.009458	−223.600449	109.6	−223.160135	95.3
		Intermediates			
a_1	0.036482	−223.911853	−68.8	−223.439781	−63.2
a_2	0.036482	−223.911853	−68.8	−223.437717	−61.9
b	0.038940	−223.913626	−68.4	−223.438966	−61.2
c	0.037733	−223.873176	−43.8	−223.392688	−32.9
d	0.039504	−223.901426	−60.4	−223.424888	−52.0
e_1	0.037669	−223.958159	−97.2	−223.487745	−92.6
e_2	0.037905	−223.961586	−99.1	−223.492155	−95.2
e_3	0.037007	−223.954831	−95.5	−223.484333	−90.9
e_4	0.037560	−223.957112	−96.6	−223.487277	−92.4
f_1	0.036937	−223.932053	−81.2	−223.456888	−73.7
f_2	0.036396	−223.922296	−75.5	−223.447196	−68.0
g	0.038020	−223.914611	−69.6	−223.436637	−60.3
h_1	0.035607	−223.866689	−41.0	−223.386703	−30.5
h_2	0.036095	−223.873075	−44.7	−223.393208	−34.3
i	0.037185	−223.944401	−88.6	−223.466621	−79.6
j	0.038781	−223.882895	−49.3	−223.404408	−39.6
k	0.037252	−223.912067	−68.5	−223.442117	−64.2
l_1	0.035681	−223.852056	−31.8	−223.380651	−26.6
l_2	0.035678	−223.855416	−33.9	−223.383513	−28.4

The initial adduct (a_1), *N*−nitrosomethanimine, is a stable and chainlike trans isomer with C_s symmetry, 63.2 kcal/mol below the reactants. Its cis isomer with C_s symmetry possesses one imaginary frequency 244i cm^{-1}, and when relaxed, it leads to another low-lying chainlike isomer (a_2) with a twisted configuration (C_1). Adduct (a_1) can isomerize to intermediate (a_2) via the rotational transition state TSa_1a_2. As shown in Figure 9, the ring closure of intermediate (a_2) may proceed to a four-membered ring intermediate (b) via transition state TSa_2b with the barrier height 34.2 kcal/mol. At the B3LYP/6-31G(d,p) level, intermediate (a_2) acts as a bridge between (a_1) and (b) via the respective transition states TSa_1a_2 and TSa_2b, confirmed by the IRC calculations. It is worthy of note that at the single-point QCISD(T)/6-311G(d,p) level, (a_2) is 0.8 kcal/mol higher in energy than TSa_1a_2, indicating either that (a_2) is not a minimum structure or that TSa_1a_2 connects other isomers instead of (a_1) and (a_2). To ascertain this problem, we further use another popular method MP2/6-31G(d,p) to optimize (a_2), TSa_1a_2 and TSa_2b. Fortunately, at the MP2/6-31G(d,p) level, all the three species do exist and have the same connection as at B3LYP/6-31G(d,p) level, which is verified by vibrational frequency and IRC calculations. The "abnormal" barrier by single-point calculations may then just indicate that (a_2) is kinetically very unstable toward isomerization.

The stable cyclic intermediate (b) may successively evolve to the other two stable four-membered ring intermediates (c) and (d) via two 1,2-hydrogen shift transition states TSbc and TScd. No direct transition state from (b) to (d) is found. The cyclic intermediate (d) can further isomerize to a chainlike intermediate (e_1) via a ring opening transition state $TSde_1$. It should be particularly pointed out that the conversion of (b) → (c) involves the high barrier of 56.3 kcal/mol. So we expect that the formation of intermediates (a_1), (a_2), and (b) is more feasible than the formation of other intermediates in this isomerization channel.

In our calculations, we found that (e_1, e_2, e_3, e_4) were the lowest lying intermediates, at least 90.9 kcal/mol below the reactants. Therefore, they each possess a high internal energy and thus may be the most activated. In terms of C-bound and N-bound hydrogens, intermediates (e_2), (e_3), and (e_4) have cis−trans, cis-cis, and trans-cis C_s symmetry structure. But intermediate (e_1) corresponds to the twisted configuration. The trans−trans planar structure of (e) has an imaginary frequency 223i cm^{-1}. It is actually a transition state TSe_1e_1 associated with

TABLE 2: Zero-Point Vibration Energies (in hartree), Total Energies (TE) (in hartree), and Relative Energies (RE) (in kcal/mol) of Transition States of Primary Reaction at the B3LYP/6-31G(d,p) and QCISD(T)/6-311G(d,p)// B3LYP/6-31G(d,p) Levels

	B3LYP/6-31G(d,p)			QCISD(T)/6-311G(d,p)// B3LYP/6-31G(d,p)TE	
TS	ZPVE	TE	RE	TE	RE
Isomerizations of Intermediates					
TSa_1j	0.035859	−223.839625	−23.9	−223.362560	−15.2
TSa_2j	0.033668	−223.805075	−3.6	−223.331453	3.0
TSa_1a_2	0.036023	−223.910892	−68.5	−223.438436	−62.7
TSa_2b	0.036723	−223.862075	−37.5	−223.385445	−29.0
TSbc	0.033664	−223.822354	−14.4	−223.344032	−4.9
TScd	0.033925	−223.823360	−14.9	−223.346338	−6.2
$TSde_1$	0.037044	−223.873352	−44.3	−223.398733	−37.1
TSe_1e_1	0.037545	−223.954008	−94.6	−223.485053	−91.0
TSe_1e_2	0.037229	−223.957754	−97.2	−223.487598	−92.8
TSe_1e_4	0.034304	−223.878753	−49.4	−223.391219	−34.1
TSe_2e_3	0.034687	−223.883156	−52.0	−223.408227	−44.6
TSe_3e_4	0.036590	−223.949917	−92.7	−223.479375	−88.0
TSe_1f_1	0.031261	−223.841468	−28.0	−223.370919	−23.3
TSe_2f_2	0.031390	−223.849349	−32.8	−223.378313	−27.9
TSe_3f_1	0.030425	−223.843904	−30.0	−223.389953	−35.8
TSf_1f_2	0.035687	−223.914454	−71.0	−223.440070	−63.9
TSe_2g	0.031516	−223.840024	−26.9	−223.356581	−14.2
TSa_2h_1	0.032341	−223.828128	−18.9	−223.351213	−10.3
TSh_1h_2	0.034906	−223.864326	−40.0	−223.385150	−30.0
TSh_2i	0.033797	−223.821444	−13.8	−223.341560	−3.3
TSa_1l_1	0.029221	−223.764186	19.3	−223.294460	23.4
TSl_1l_2	0.031511	−223.777463	12.4	−223.298850	22.1
TSjk	0.032380	−223.777463	13.5	−223.300501	21.6
Transition states of dissociations of intermediates					
$TSbP_1$	0.035419	−223.870050	−43.3	−223.396741	−36.9
TSe_1P_1	0.029963	−223.842533	−29.4	−223.387089	−34.3
TSe_4P_1	0.031396	−223.883323	−54.1	−223.409822	−47.6
TSf_1P_1	0.030513	−223.875117	−49.5	−223.398740	−41.2
TSR_cP_1	0.033203	−223.800018	−0.71	−223.327559	5.1
TSe_3P_2	0.031782	−223.918346	−75.9	−223.445932	−70.1
TSf_2P_2	0.031413	−223.895083	−61.5	−223.420718	−54.5
TSP_1P_3	0.030658	−223.849036	−33.1	−223.849036	−35.0
TSa_1P_4	0.029548	−223.852125	−35.7	−223.383616	−32.4
$TSdP_4$	0.034653	−223.782375	11.3	−223.302991	21.4
$TSkP_4$	0.031748	−223.855845	−36.7	−223.382092	−30.0
TSl_2P_4	0.032010	−223.838814	−25.8	−223.376843	−26.6
TSP_4P_5	0.031778	−223.768591	18.1	−223.294696	24.8
TSa_2P_6	0.033046	−223.838819	−25.2	−223.389450	−33.8
$TScP_7$	0.035155	−223.797081	2.35	−223.323691	8.8
TSe_2P_7	0.031352	−223.898010	−63.4	−223.426212	−57.9
$TSdP_8$	0.034280	−223.756100	27.5	−223.281540	34.7
TSe_4P_8	0.031121	−223.856590	−37.5	−223.378638	−28.2
TSf_2P_8	0.031851	−223.897131	−62.5	−223.424869	−56.8
$TSiP_8$	0.030884	−223.822603	−16.8	−223.347191	−8.7
$TSgP_9$	0.030881	−223.851235	−34.3	−223.381358	−30.1
TSe_4P_{10}	0.027788	−223.920275	−79.6	−223.451442	−76.0
TSf_1P_{10}	0.026661	−223.885951	−58.7	−223.414157	−53.3

the automerization of (e_1) with a very small barrier of 1.6 kcal/mol.

Starting from (e_1), two bond rotation transition states TSe_1e_2 and TSe_1e_4 were located, while no transition state for the conversion of (e_1)→(e_3) was found. In addition, the C−N single bond rotation transition state TSe_3e_4 and N═N double bond rotation transition state TSe_2e_3 were also located. In contrast, the N═N bond rotation transition state TSe_2e_3 involves a barrier at least 40.0 kcal/mol higher than that of the C−N single bond rotation transition state TSe_1e_2 and TSe_3e_4. The conversion of (e_1)→(e_4) is a concerted process of C−N bond and N═N bond rotations via the transition state TSe_1e_4 with the high barrier of 58.5 kcal/mol. The conversion of (e_1)→(e_3) also requires undergoing such a concerted process and surmounting a high barrier. As a result, we expect that a stepwise conversion process (e_1)→(e_2)→(e_3) must be more feasible than the direct conversion process (e_1)→(e_3). In conclusion, the formation of (e_3) and (e_4) is very difficult due to the high barriers of TSe_2e_3 and TSe_1e_4. It should be noted that when ZPVEs are included, the intermediate (e_1) has the same energy as TSe_1e_2 at the B3LYP/6-31G(d,p) level and is even 0.2 kcal/mol above TSe_1e_2 at the QCISD(T)/6-311G(d,p) level. However, the additional MP2/6-31G(d,p) calculations confirm the connection of TSe_1e_2 between e_1 and e_2. Also, $TSde_1$ and TSe_1e_4 are shown to be connected with e_1 at the MP2/6-31G(d,p) level. Then, the fact that (e_1) is slightly higher in energy than TSe_1e_2 is just a result of single-point calculations. Yet, this at least means that intermediate (e_1) is unstable even at 0 K.

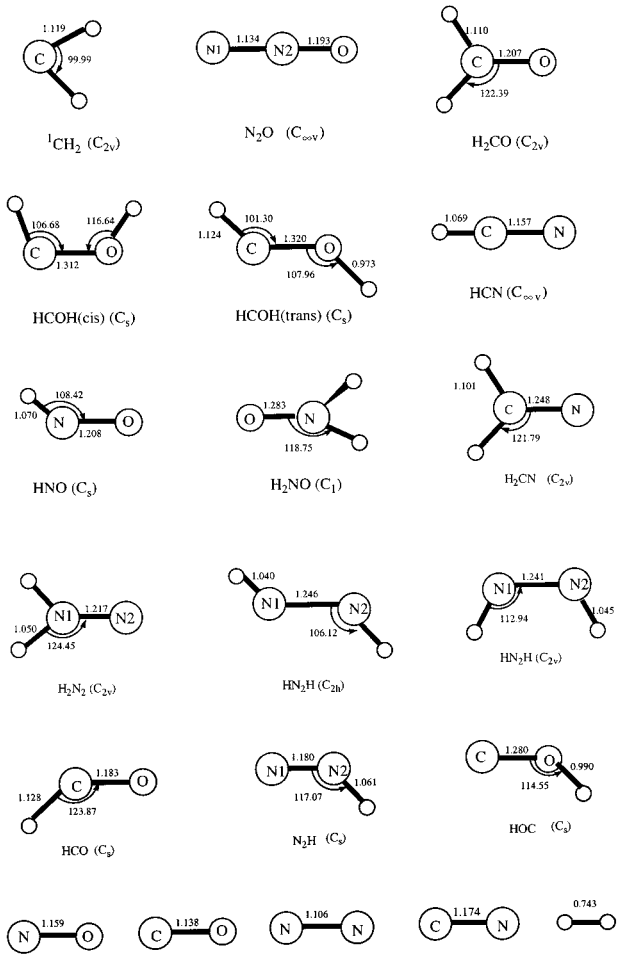

Figure 7. Geometries of reactants and products at the B3LYP/6-31G-(d,p) level. Bond lengths are in angstroms and bond angles in degrees.

TABLE 3: Zero-Point Vibration Energies (in hartree), Total Energies (TE) (in hartree), and Relative Energies (RE) (in kcal/mol) of Transition States of Secondary Reactions and Corresponding to Fragments at the B3LYP/6-31G(d,p) and QCISD(T)/6-311G(d,p)//B3LYP/6-31G(d,p) Levels

	B3LYP/6-31G(d,p)			QCISD(T)/6-311G(d,p)// B3LYP/6-31G(d,p)	
species	ZPVE	TE	RE	TE	RE
$TSP_1P_2+N_2$	0.026221	−223.887196	−59.8	−223.433803	−65.9
$TSP_3P_2+N_2$	0.027903	−223.891804	−61.6	−223.438481	−67.8
$TSP_1P_{10}+N_2$	0.024471	−223.889059	−62.1	−223.434417	−67.4
$TSP_2P_{10}+N_2$	0.022869	−223.849247	−38.1	−223.397937	−5.5
TSP_6P_{13}+NO	0.021866	−223.809040	−13.5	−223.351883	−17.3
TSP_7P_8+CO	0.025732	−223.832195	−25.6	−223.377196	−30.7
TSP_7P_9+CO	0.025248	−223.794968	−2.5	−223.337208	−5.9
TSP_8P_9+CO	0.028439	−223.849194	−34.6	−223.392653	−38.7
TS_7P_{12}+CO	0.024134	−223.823990	−21.5	−223.349918	−14.6
TS_9P_{10}+CO	0.021217	−223.791142	−2.7	−223.339443	−9.9

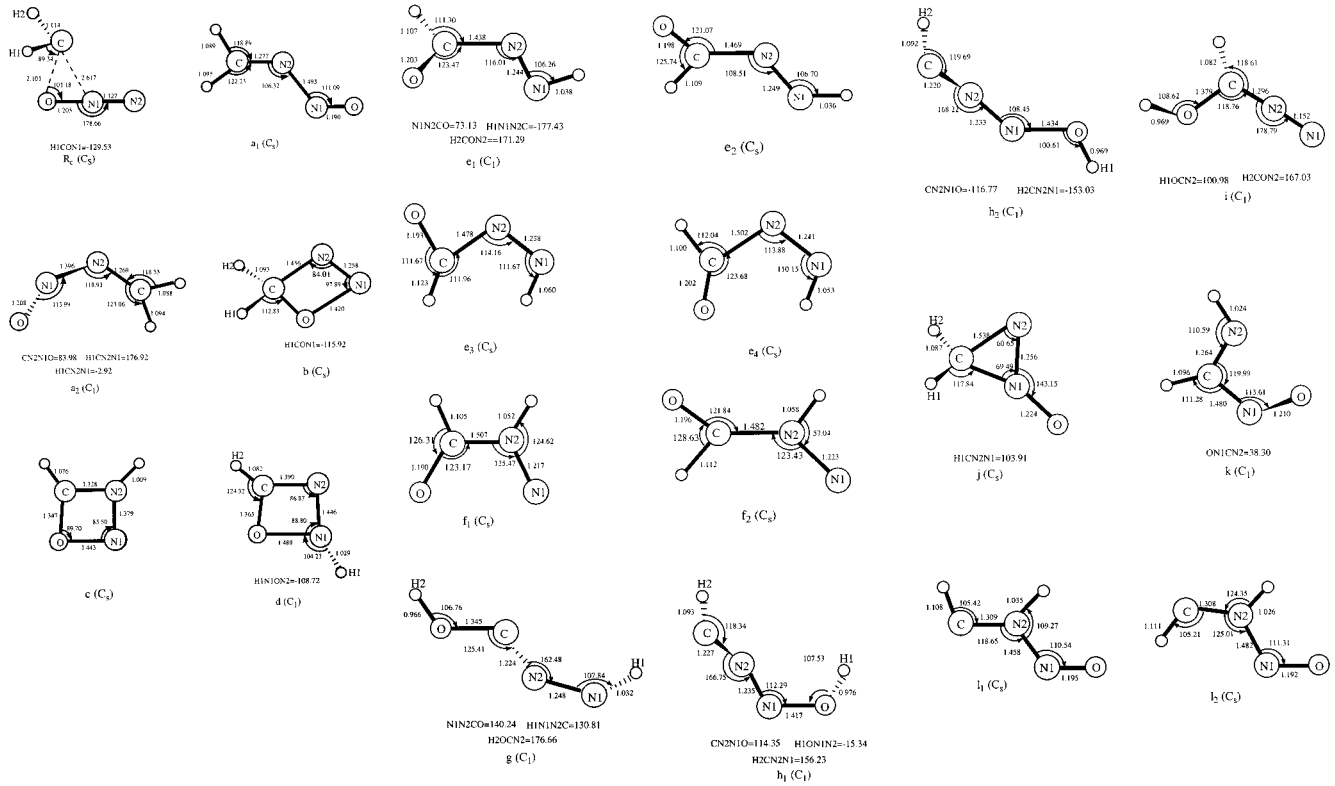

Figure 8. Geometries of intermediate at the B3LYP/6-31G(d,p) level. Bond lengths are in angstroms and bond angles in degrees.

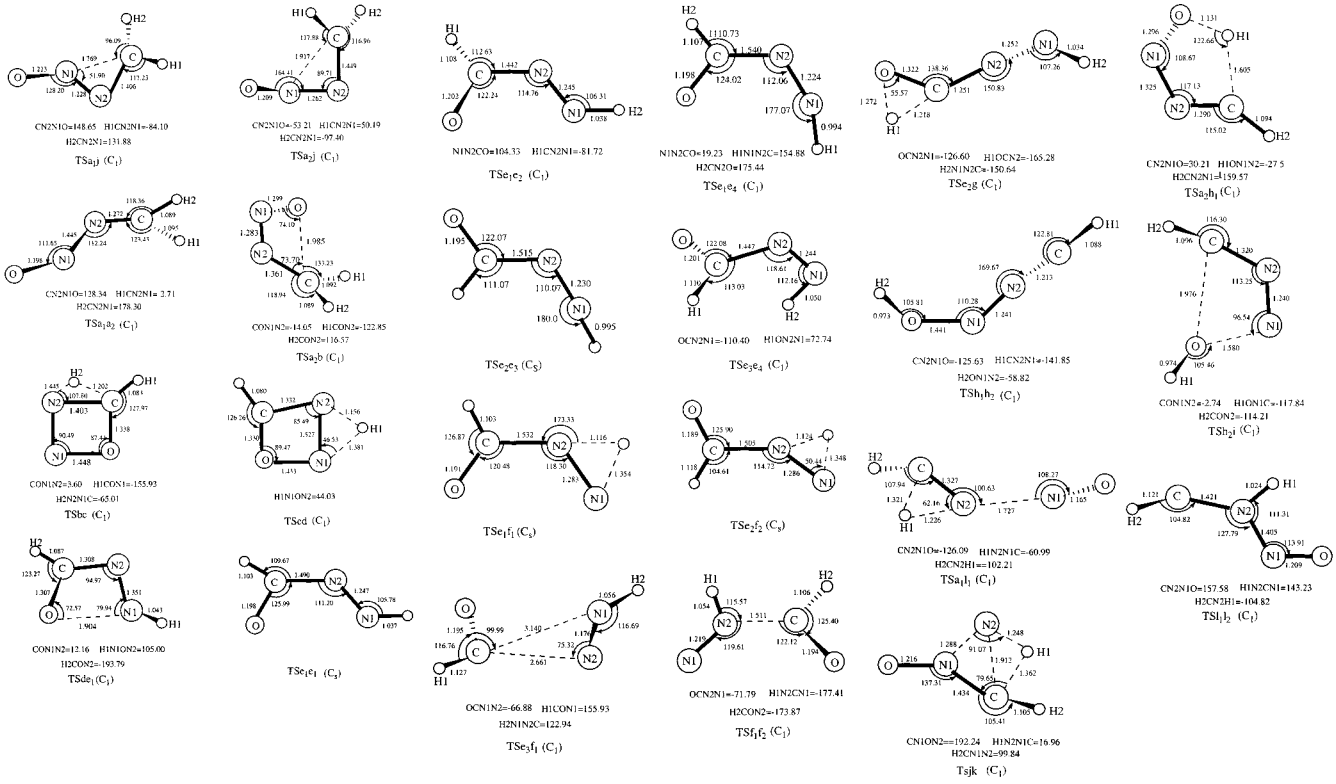

Figure 9. Geometries of the transition states of isomerization at the B3LYP/6-31G(d,p) level. Bond lengths are in angstroms and bond angles in degrees.

As shown in the potential energy surfaces, three isomerization channels from (e) to (f) are obtained. The first channel is a 1,2-hydrogen migration via TSe_1f_1 with the high barrier of 69.3 kcal/mol. As seen in Figure 9, TSe_1f_1 has a tight three-membered ring structure. The migrating hydrogen is 1.354 Å away from the origin and 1.116 Å away from the migrating terminus. The second channel undergoes migration via a 1,2-hydrogen shift transition state TSe_2f_2 (67.3 kcal/mol) with a structure similar to TSe_1f_1. The last channel is the formation of (f_1) from (e_3) when the C-atom of the HCO group migrates from the outside N-atom (N2) to the inner N-atom (N1) of the NNH group along with a concerted twist as illustrated by IRC calculations. The transition state TSe_3f_1 has a loose three-membered ring structure with surprisingly long C−N distances, i.e., r(CN1) = 3.140 Å

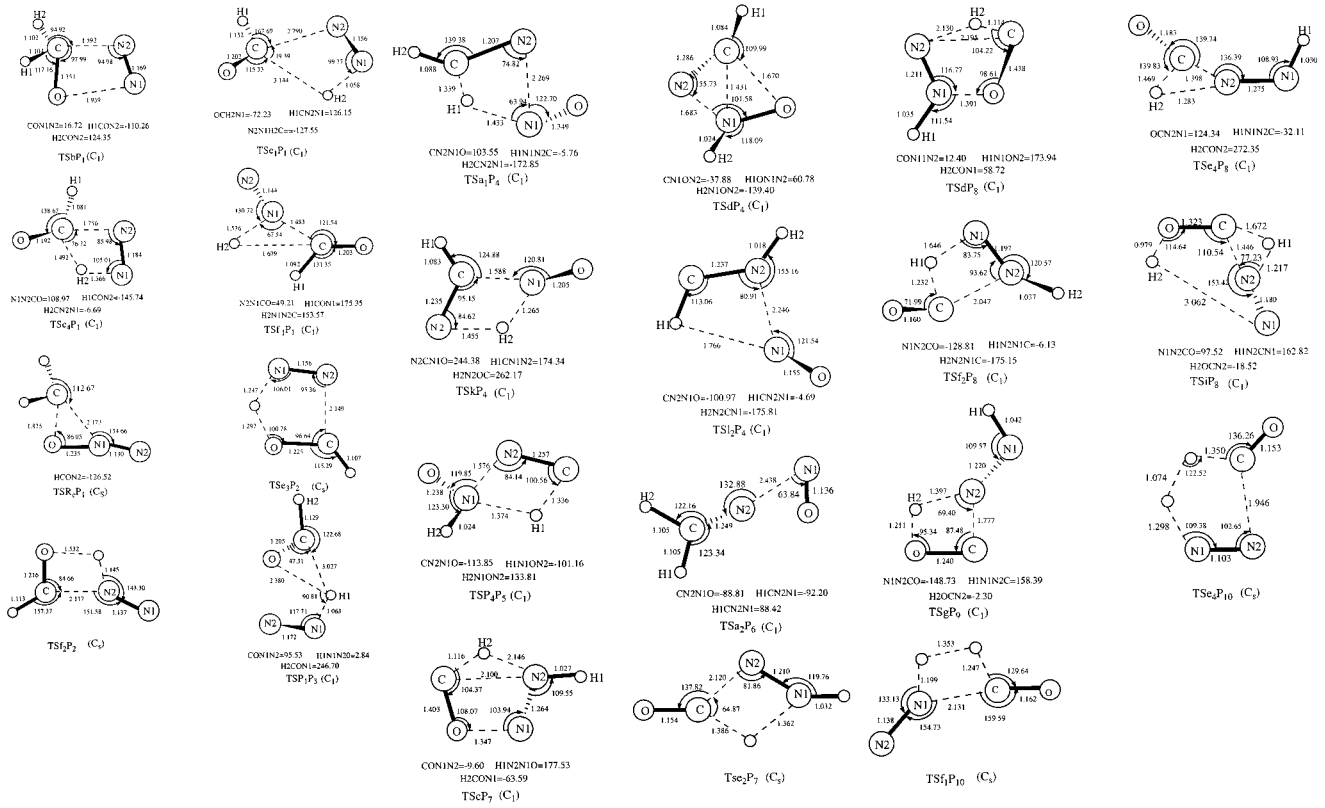

Figure 10. Geometries of the transition states of dissociation at the B3LYP/6-31G(d,p) level. Bond lengths are in angstroms and bond angles in degrees.

and r(CN2) = 2.661 Å. The $(e_3)\rightarrow(f_1)$ conversion barrier is rather high, 55.1 kcal/mol, which is even 16.8 kcal/mol higher than the direct dissociation of (e_3) to product $P_{11}(N_2H+HCO)$. The imaginary frequency of 241i cm^{-1} mainly involves a N···C(OH)···N bending motion. Because (f) is obtained via three high barrier transition states, the formation of (f) is very difficult.

Intermediates (f_1) and (f_2), which are cis and trans isomers in terms of hydrogen atoms, are still very low-lying intermediates. The interconversion between them takes place via a C−N single bond rotation transition state TSf_1f_2. The process involves a low internal rotation barrier (9.8 kcal/mol above (f_1)) because of the long C−N single bond length ((f_1) 1.507 Å, (f_2) 1.482 Å). We tried to locate the transition state from (b) to (f_1), yet all of our attempts invariably led to TSf_1f_2. The $(e_2)\rightarrow(g)$ conversion is a 1,2-hydrogen migration process through a three-membered ring transition state TSe_2g with a large barrier (84.9 kcal/mol).

Channel (i2) is another isomerization pathway starting from (a_1). First, $(a_2)\rightarrow(h_1)$ is a 1,4-hydrogen migration process via the five-membered ring transition state TSa_2h_1. TSa_2h_1 surmounts the barrier of 51.6 kcal/mol, entering a relatively shallow potential well. The intermediates (h_1) and (h_2) are trans and cis isomers connected by the transition state TSh_1h_2 with a small internal rotation barrier. Isomerization from (h_2) to the very low-lying intermediate (i) undergoes 1,3-migration of the OH group through TSh_2i, forming (i) after clearing the barrier of 31.0 kcal/mol. The calculation of Michael et al.[16] indicated that the twisted OH group conformation (namely, (i)) was energetically more stable than that with a coplanar OH group. Our calculation is in good agreement with their result.

Channel (i3) undergoes two isomerization processes. The first step is 1,2-hydrogen migration via transition TSa_1l_1 with the high barrier of 88.1 kcal/mol, giving rise to intermediate (l_1). The second step is the conversion from $l_1\rightarrow l_2$ via C−N2 bond rotation transition state TSl_1l_2. Because the C−N2 bond in (l_1) or (l_2) has partial double bond character, the internal rotational barrier is very high (48.7 kcal/mol).

Channel (i4) can be rationalized in terms of a single-step process of isomerization. The low-lying three-membered ring structure (j) may evolve to intermediate (k) through a transition state TSjk. This is a 1,2-hydrogen migration process, along with the concerted ring opening. The process involves a high barrier of 62.1 kcal/mol, and TSjk is even 22.1 kcal/mol above the reactants. This may be attributed partly to the steric strain of two adjacent three-membered rings. Except for (j)→(a) and (j)→(k) conversions, no other isomerization pathways of (j) can be found.

3.3. Dissociation Channels. *3.3.1. Channels Related to Primary Products P_1 (N_2+H_2CO) and P_2 (N_2+HCOH(trans)).* Let us first examine the following reaction channels:

$$R\rightarrow a_1\rightarrow a_2\rightarrow b\rightarrow P_1(N_2+H_2CO) \quad (r1)$$

$$R\rightarrow a_1\rightarrow a_2\rightarrow b\rightarrow c\rightarrow d\rightarrow e_1\rightarrow P_1(N_2+H_2CO) \quad (r2)$$

$$R\rightarrow a_1\rightarrow a_2\rightarrow b\rightarrow c\rightarrow d\rightarrow e_1\rightarrow e_4\rightarrow P_1(N_2+H_2CO) \quad (r3)$$

$$R\rightarrow a_1\rightarrow a_2\rightarrow b\rightarrow c\rightarrow d\rightarrow e_1\rightarrow f_1\rightarrow P_1(N_2+H_2CO) \quad (r4)$$

$$R_c\rightarrow P_1(N_2+H_2CO) \quad (r5)$$

$$R\rightarrow a_1\rightarrow a_2\rightarrow b\rightarrow c\rightarrow d\rightarrow e_1\rightarrow e_2\rightarrow e_3\rightarrow P_2(N_2+HCOH(trans)) \quad (r6)$$

$$R\rightarrow a_1\rightarrow a_2\rightarrow b\rightarrow c\rightarrow d\rightarrow e_1\rightarrow e_2\rightarrow f_2\rightarrow P_2(N_2+HCOH(trans)) \quad (r7)$$

The channel (r1) of $P_1(N_2+H_2CO)$ is a cyclic elimination of N_2 along with the formation of H_2CO via transition state $TSbP_1$ with 24.3 kcal/mol activation energy. The tight four-membered ring structure $TSbP_1$ is characterized by slightly elongated C−N and N−O bonds and compressed N−N and C−O bonds. The

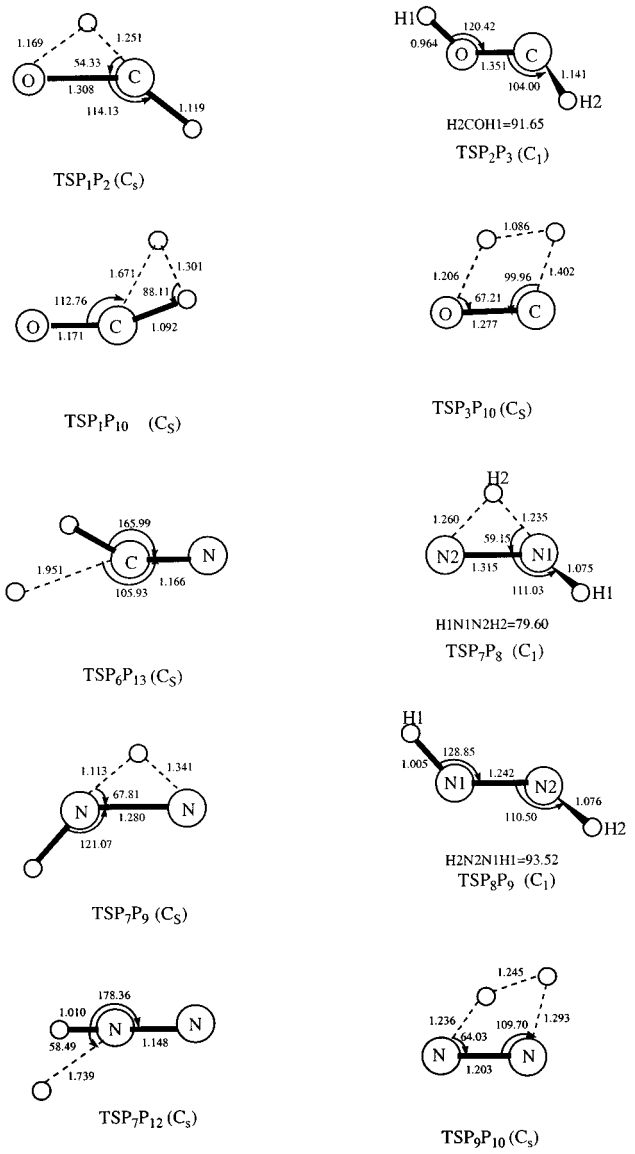

Figure 11. The geometries of the transition states of isomerization and dissociations of fragments at the B3LYP/6-31G(d,p) level. Bond lengths are in angstroms and bond angles in the degrees.

analysis of this transition structure indicates that vibrationally excited H_2CO and vibrationally cold N_2 are formed.

For the channels (r2) and (r3), we investigated the 1,3-hydrogen migration in (e) and obtained the transition states TSe_1P_1 (58.3 kcal/mol) and TSe_4P_1 (44.6 kcal/mol). Both of the migrations are associated with a cleavage of the C−N2 single bond. As shown in Figure 10, TSe_1P_1 presents a very loose four-membered ring structure, which is highly nonplanar. The distances of C−N2 and C−H2 are surprisingly long as 2.790 Å and 3.144 Å, respectively, while the N1−H2 bond that will be broken is surprisingly short as 1.058 Å. Despite the abnormal structure, TSe_1P_1 is confirmed to be a first-order saddle point with a large imaginary frequency 312i cm^{-1} and it connects (e_1) and P_1 tested by our IRC calculations. The fourth formation channel (r_4) of P_1 is a concerted C−N2 bond cleavage and hydrogen migration process via a three-membered ring transition state TSf_1P_1.

The last formation channel (r5) of P_1 is found to be a direct abstraction process. The O atom in N_2O is abstracted by the C atom in $^1CH_2$, forming the products H_2CO and N_2. The transition state TSR_cP_1 can be considered as an "early" saddle point. Compared with the bond lengths of reactant N_2O, the N−N bond length in TSR_cP_1 is almost unchanged, whereas the N−O bond is just slightly elongated. At the 6-31G(d,p) MP2 and B3LYP levels, TSR_cP_1 is optimized to be energetically disposed at 7.4 and 0.71 kcal/mol, respectively, below the reactants. This suggests an initial formation of a π-complex between $^1CH_2$ and N_2O, followed by displacement of N_2. In fact, such a complex was obtained at the B3LYP/6-31G(d,p) level lying 3.2 kcal/mol below the reactants. Further QCISD(T)/6-311G(d,p) single-point calculations show that the $R_c \rightarrow P_1$ conversion process requires clearing the low barrier of 6.0 kcal/mol. The large internal energy 154.1 kcal/mol of P_1 gained from this process can then be rapidly distributed into the appropriate vibrational modes to form P_1.

Now let us compare which is the most probable formation channel of product $P_1(N_2+H_2CO)$. Among the channels (r1)−(r4), (r1) involves the fewest intermediates. Also, the barrier for (b)→P_2 conversion in (r1) is much smaller (by 32.0 kcal/mol) than that for (b)→(c) conversion in other channels. Therefore, (r1) is expected to be the most feasible channel for $P_1(N_2+H_2CO)$. The channel (r5) is surely much less competitive owing to the high-energy transition state above the reactants, though it is a direct process. However, since the direct O-abstraction barrier is just 5.1 kcal/mol above the reactants, (r5) may become feasible at high temperatures.

Now we turn to the formation of $P_2(N_2+HCOH(trans))$. The channels (r6) and (r7) both involve intermediate (e_2). Though their dissociation barriers are very low, (e_2)→(e_3) in channel (r6) and (e_2)→(f_2) in channel (r7) require surmounting high barriers, i.e., 50.6 and 67.3 kcal/mol, respectively. Thus, the formation of P_2 plays an unimportant role in the reaction kinetics.

The secondary reactions of the primary products P_1 (N_2+H_2-CO) were considered. P_1 can convert to P_2, P_3 (N_2+HCOH-(cis)), P_{10} (N_2+H_2+CO) and P_{14} (N_2+HCO+H). The process from P_1 to P_2 is associated with the $H_2CO \leftrightarrow$HCOH (trans) isomerization, whereas the processes from P_1 to P_{10} and P_{14} are, respectively, H_2- and H-elimination of H_2CO. The process from P_1 to P_3 can be considered as an interesting N_2-assisted $H_2CO \leftrightarrow$HCOH (cis) isomerization. Unfortunately, all of the four secondary conversions of P_1 have to overcome very high barriers (more than 80 kcal/mol). Thus, P_1 (N_2+H_2CO) may be considered as the final product.

3.3.2. Channels Related to Primary Products P_4 (HCN+HNO) and P_5 (NO+H_2CN). From Figure 4, we sum up the reaction channels for P_4 (HNO+HCN) and P_5 (NO+H_2CN) as follows:

$$R \rightarrow a_1 \rightarrow P_4\,(HNO+HCN) \qquad (r8)$$

$$R \rightarrow a_1 \rightarrow a_2 \rightarrow b \rightarrow c \rightarrow d \rightarrow P_4\,(HNO+HCN) \qquad (r9)$$

$$R \rightarrow j \rightarrow k \rightarrow P_4\,(HNO+HCN) \qquad (r10)$$

$$R \rightarrow a_1 \rightarrow a_2 \rightarrow l_1 \rightarrow l_2 \rightarrow P_4\,(HNO+HCN) \qquad (r11)$$

$$R \rightarrow a_1 \rightarrow a_2 \rightarrow P_5\,(NO+H_2CN) \qquad (r12)$$

Clearly, because the transition states $TSdP_4$, TSa_1l_1, and TSjk in channel (r9), (r10), and (r11) lie significantly above reactants and must surmount very high barriers, all three channels are negligible in the reaction dynamics for P_4. So only channel (r8) is the feasible for formation of P_4. In (r8), (a_1) can take a direct dissociation to P_4 through a concerted 1,3-hydrogen migration and N−N bond cleavage process via the dissociation transition state TSa_1P_4. The product P_5 (NO+H_2CN) is formed via the direct cleavage transition state TSa_2P_5 in channel (r12). The

process from (a) to P_5 involves activation energy of 29.4 kcal/mol.

The species HNO in P_4 and H_2CN in P_5 may further lose an H atom to give NO and HCN, respectively. The dissociation of H_2CN to H+HCN needs a barrier 29.3 kcal/mol via TSP_5P_{13}. In addition, the N−H simple bond fission of HNO produces H+NO with endothermicities of 41.9 kcal/mol. We also locate a transition state TSP_4P_6 for the H-abstraction from HCN to HNO in P_4 to form P_6 (CN+H_2NO). Yet, TSP_4P_6 lies 24.8 kcal/mol above the reactants and the process is impossible. Moreover, the products P_{17} (HNO+CN+H) and P_{18} (NO+CN+2H) lie 53.4 and 89.9 kcal/mol above reactants (see Table 1), respectively. These product channels are unimportant for the reaction dynamics.

3.3.3. Channels Related to Primary Products P_7 (CO+H_2N_2), P_8 (CO+HN_2H (trans)), and P_9 (CO+HN_2H (cis)). Let us investigate the following reaction channels:

$$R\rightarrow a_1\rightarrow a_2\rightarrow b\rightarrow c\rightarrow P_7\,(CO+H_2N_2) \quad \text{(r13)}$$

$$R\rightarrow a_1\rightarrow a_2\rightarrow b\rightarrow c\rightarrow d\rightarrow e_1\rightarrow e_2\rightarrow P_7\,(CO+H_2N_2) \quad \text{(r14)}$$

$$R\rightarrow a_1\rightarrow a_2\rightarrow b\rightarrow c\rightarrow d\rightarrow P_8\,(CO+HN_2H\ (trans)) \quad \text{(r15)}$$

$$R\rightarrow a_1\rightarrow a_2\rightarrow b\rightarrow c\rightarrow d\rightarrow e_1\rightarrow e_4\rightarrow P_8\,(CO+HN_2H\ (trans)) \quad \text{(r16)}$$

$$R\rightarrow a_1\rightarrow a_2\rightarrow b\rightarrow c\rightarrow d\rightarrow e_1\rightarrow e_2\rightarrow f_2\rightarrow P_8(CO+HN_2H\ (trans)) \quad \text{(r17)}$$

$$R\rightarrow a_1\rightarrow a_2\rightarrow h_1\rightarrow h_2\rightarrow i\rightarrow P_8\,(CO+HN_2H\ (trans)) \quad \text{(r18)}$$

$$R\rightarrow a_1\rightarrow a_2\rightarrow b\rightarrow c\rightarrow d\rightarrow e_1\rightarrow e_2\rightarrow g\rightarrow P_9\,(CO+HN_2H\ (cis)) \quad \text{(r19)}$$

Channels (r13) and (r15) are surely impossible because the involved transition states $TScP_7$ and $TSdP_8$ lie higher than the reactants. The remaining channels can be sorted into two groups considering different isomers. Channels (r14), (r16), (r17), and (r19) proceed via the intermediates (a), (b), (c), (d), and (e), while (r20) proceeds via the intermediates (a), (h), and (i). The isomer (e_2) has several conversion processes. The dissociation of (e_2) can either directly lead to P_7, or indirectly to P_8 and P_9 via the intermediates (f) and (g), respectively. Since the conversion barrier from (e_2) to P_7 is much lower than those from (e_2) to (f_2) and (e_2) to (g), channel (r14) is much more feasible than (r17) and (r19). In addition, the conversion of (e_1)→(e_4) requires the high barrier of 58.5 kcal/mol. It is expected that (r16) is unimportant for the formation of P_8. Since the highest barrier (70.9 kcal/mol from (i) to P_8) in (r18) is much larger than that (56.3 kcal/mol from (b) to (c)) in (r14), we expect that P_7 may be a more competitive product than P_8.

In view of the secondary reactions, the barrier height from P_7 to P_8 is 47.5 kcal/mol. Yet, the barriers from P_7 to P_9 and P_{12} are rather high as 72.3 and 63.6 kcal/mol, making the processes less likely. The conversion from P_8 to P_9 is also difficult because of the barrier 64.8 kcal/mol. The products P_{10} and P_{15} are almost impossible.

3.3.4. Channels Related to Primary Products P_{10} (CO+N_2+H_2) and P_{11} (N_2H+HCO). We found two reaction channels of dissociation to products P_{10} (CO+N_2+H_2):

$$R\rightarrow a_1\rightarrow a_2\rightarrow b\rightarrow c\rightarrow d\rightarrow e_1\rightarrow e_4\rightarrow P_{10}\,(CO+N_2+H_2) \quad \text{(r20)}$$

$$R\rightarrow a_1\rightarrow a_2\rightarrow b\rightarrow c\rightarrow d\rightarrow e_1\rightarrow e_2\rightarrow f_2\rightarrow P_{10}\,(CO+N_2+H_2) \quad \text{(r21)}$$

Based on the collision theory, the collision and reaction probability of three molecules is very low. However, we located two low barrier transition states for direct dissociation to product P_{10} (CO+N_2+H_2), namely, TSe_4P_{10} (16.4 kcal/mol) and TSf_1P_{10} (20.4 kcal/mol). Both channels represent the same process of simultaneous H,H elimination and the cleavage of the C−N2 bond. However, the channel (r20) is more feasible than (r21) for the formation of P_{10}(CO+N_2+H_2) because the conversion barrier from (e_2) to (f_2) is higher than that from (e_1) to (e_4).

For the formation of P_{11} (N_2H+HCO), three channels were obtained as (r22) → (r24):

$$R\rightarrow a_1\rightarrow a_2\rightarrow b\rightarrow c\rightarrow d\rightarrow (e_1, e_2)\rightarrow P_{11}\,(N_2H+HCO) \quad \text{(r22)}$$

$$R\rightarrow a_1\rightarrow a_2\rightarrow b\rightarrow c\rightarrow d\rightarrow (e_1, e_2)\rightarrow (e_3,e_4)\rightarrow P_{11}\,(N_2H+HCO) \quad \text{(r23)}$$

$$R\rightarrow a_1\rightarrow a_2\rightarrow b\rightarrow c\rightarrow d\rightarrow e(e_1\ e_2\ e_3\ e_4)\rightarrow f\,(f_1,f_2)\rightarrow P_{11}\,(N_2H+HCO) \quad \text{(r24)}$$

These three channels are associated with the simple bond cleavage of intermediates e(e_1, e_2, e_3, e_4) and f(f_1, f_2) without surmounting the well-defined transition states. As discussed in section 3.1, (e_3), (e_4), (f_1), and (f_2) are more difficult to obtain than (e_1) and (e_2), so we expect that channel (r22) may be much more competitive than (r23) and (r24). The secondary dissociation from P_{11} to P_{14} and P_{15} can proceed almost without barriers once P_{11} is formed.

3.4. Reaction Mechanism. In the preceding sections, we have discussed various reaction channels for possible primary products of the reaction $^1CH_2$+N_2O. For easy comparison, the most feasible channels for the primary products are listed again. The feasible secondary dissociation products are also included.

$$\underline{\mathbf{R\rightarrow a_1\rightarrow a_2\rightarrow b\rightarrow P_1(N_2+H_2CO)}} \quad \text{(r1)}$$

$$R\rightarrow a_1\rightarrow a_2\rightarrow b\rightarrow c\rightarrow d\rightarrow e_1\rightarrow e_2\rightarrow e_3\rightarrow P_2(N_2+HCOH(trans))\rightarrow P_{14}(N_2+HCO+H)\rightarrow P_{15}(N_2+2H+CO)$$

or

$$R\rightarrow a_1\rightarrow a_2\rightarrow b\rightarrow c\rightarrow d\rightarrow e_1\rightarrow e_2\rightarrow e_3\rightarrow P_2(N_2+HCOH(trans))\rightarrow P_1(N_2+HCO+H)$$

or

$$R\rightarrow a_1\rightarrow a_2\rightarrow b\rightarrow c\rightarrow d\rightarrow e_1\rightarrow e_2\rightarrow e_3\rightarrow P_2(N_2+HCOH(trans))\rightarrow P_3(N_2+HCOH(\textit{trans}))\rightarrow P_{14}(N_2+HCO+H)\rightarrow P_{15}(N_2+2H+CO) \quad \text{(r6)}$$

$$\underline{\mathbf{R\rightarrow a_1\rightarrow P_4\,(HNO+HCN)\rightarrow P_{13}(NO+HCN+H)}} \quad \text{(r8)}$$

$$\underline{\mathbf{R\rightarrow a_1\rightarrow a_2\rightarrow P_5\,(NO+H_2CN)\rightarrow P_{13}(NO+HCN+H)}} \quad \text{(r12)}$$

$$R\rightarrow a_1\rightarrow a_2\rightarrow b\rightarrow c\rightarrow d\rightarrow e_1\rightarrow e_2\rightarrow P_7(CO+H_2N_2) \quad \text{(r14)}$$

$$R\rightarrow a_1\rightarrow a_2\rightarrow b\rightarrow c\rightarrow d\rightarrow e_1\rightarrow e_4\rightarrow P_8(CO+HN_2H(trans)) \quad \text{(r16)}$$

$$R\rightarrow a_1\rightarrow a_2\rightarrow b\rightarrow c\rightarrow d\rightarrow e_1\rightarrow e_2\rightarrow g\rightarrow P_9\,(CO+HN_2H\ (cis)) \quad \text{(r19)}$$

$$R\rightarrow a_1\rightarrow a_2\rightarrow b\rightarrow c\rightarrow d\rightarrow e_1\rightarrow e_4\rightarrow P_{10}(CO+N_2+H_2) \quad \text{(r20)}$$

$$R\rightarrow a_1\rightarrow a_2\rightarrow b\rightarrow c\rightarrow d\rightarrow (e_1, e_2)\rightarrow P_{11}\,(N_2H+HCO)\rightarrow P_{14}(N_2+HCO+H)\rightarrow P_{15}(N_2+2H+CO)$$

or

$$R \rightarrow a_1 \rightarrow a_2 \rightarrow b \rightarrow c \rightarrow d \rightarrow (e_1,e_2) \rightarrow P_{11}(N_2H+HCO) \rightarrow P_{15}(N_2+2H+CO) \quad (r22)$$

The three most feasible channels (r1), (r8), and (r12) involve simple isomerization processes with relatively low barriers. For distinction, the three channels are underlined and in bold. The remaining channels (r6), (r14), (r16), (r19), (r20), (r22) proceed through more complex intermediates with much larger barriers and higher-energy transition states. For example, the transition state TSbc (−4.9 kcal/mol) and TScd (−6.2 kcal/mol) in channel (r14) are energetically much higher than TSa_2b (−29.0 kcal/mol) in channel (r1). Moreover, the b→c conversion barrier 56.3 kcal/mol in (r14) is considerably larger than a_2→b conversion barrier 32.9 kcal/mol in (r1). Then the channels (r6), (r14), (r16), (r19), (r20), and (r22) may play a negligible role in the reaction kinetics. For the channels (r1), (r8), and (r12), the isomerization barrier from (a_2) to (b) in (r1) is at least 3.4 kcal/mol larger than the dissociation barriers of a_1→P_4 in channel (r8) and (a_2)→P_5 in channel (r12). So we expect that channels (r8) and (r12) are more competitive than channel (r1). Last, we consider the channels (r8) and (r12). It should be noticed that the energy of the transition state TSa_1P_4 in (r8) is just 1.4 kcal/mol higher than that of the transition state TSa_2P_5 in (r12). After the primary products P_4 and P_5 are formed, they can further dissociate to the same product P_{13}. Hence, we expect that channels (r8) and (r12) exist in a competitive involvement.

In addition, the channel R_c→$P_1(N_2+H_2CO)$ (r5) is a direct abstraction process with the low barrier of 6.0 kcal/mol. However, the higher-energy transition state TSR_cP_1 lies above reactants. So the direct abstraction process may become feasible only at high temperatures.

In conclusion, the formation of products P_1 (N_2+H_2CO) and P_{13} (NO+HCN+H) is favorable for the reaction kinetics. The other products, including CO and H_2, may be obtained at very low probability. We expect that the products N_2, H_2CO, NO, HCN, and H can be observed in the experiments.

4. Conclusions

Electronic structure calculations are performed to characterize the reaction between $^1CH_2$ and N_2O on the lowest singlet potential energy surface. The association $^1CH_2$ with N_2O was found to be a barrierless process forming an energy-rich adduct (a_1). Energetically, the branching ratio of P_{13} is larger than that of P_1. Our calculations show that the product P_1 (N_2+H_2CO) and P_{13} (NO+HCN+H) are the dominant products for the title reaction, whereas the other products, including CO and H_2, are minor. The product P_1 can be obtained through R→a_1→a_2→b→$P_1(N_2+H_2CO)$ (r1), whereas the product P_{13} can be obtained through two competitive channels R→a_1→P_4(HNO+HCN)→P_{13}(NO+HCN+H) (r8) and R→a_1→a_2→P_5(NO+H_2CN)→P_{13}(NO+HCN+H) (r12). We expect that the probability of obtaining P_{13} is greater than that of obtaining P_1. At high temperatures, a direct abstraction channel leading to the N_2+H_2-CO products becomes a possible channel. Our work can assist experiments to identify the products of the $^1CH_2+N_2O$ reaction.

Acknowledgment. This work is supported by the National Natural Science Foundation of China (G29892168).

References and Notes

(1) Winter, N. W. *Chem. Phys. Lett*. **1975**, *33*, 300.
(2) Laufer, A. H. *Rev. Chem. Intermed*. **1981**, *4*, 225.
(3) Homann, K. H; Schweinfurth, H. *Ber. Bunsen-Ges. Pyhs. Chem*. **1981**, *85*, 569.
(4) Homann, K. H.; Schweinfurth, H. *Ber. Bunsen-Ges. Pyhs.Chem*. **1983**, *87*, 609.
(5) Bell, T. N.; Fara, F. *Res. Chem. Intermed*. **1989**, *12*, 269.
(6) Su, H.; Yang, J.; Zhong, J.; Kong, F. *Chem. Phys. Lett*. **1999**, *303*, 526.
(7) Koch, M.; Temps, F; Wagener, R.; Wagner, H. Gg. *Ber. Bunsen-Ges. Phys. Chem.* **1990**, *94*, 645.
(8) Schlegel, H. B. *J. Chem. Phys*. **1986**, *84*, 4530.
(9) Becke, A. D. *J. Chem. Phys.* **1993**, *98*, 1372.
(10) Lee, C.; Yang, W.;Parr, R. G. *Phys. Rev.* B **1988**, *41*, 785.
(11) Gonzalez, C.; Schlegel, H. B. *J. Chem. Phys.* **1989**, *90*, 2154.
(12) Gonzalez, C.; Schlegel, H. B. *J. Chem. Phys*. **1990**, *94*, 5523.
(13) Pople, J. A.; Head-Gordon, M.; Raghavachari, K. *J. Chem. Phys.* **1987**, *87*, 5968.
(14) Knowles, P. J.; Werner, H. J. *Chem. Phys. Lett.* **1985**, *115*, 259.
(15) Harcourt, R. D.; Hall, N. *J. Mol. Struct.* **1995**, *342*, 59.
(16) McAllister, M. A.; Tidwell, T. T. *J. Am. Chem. Soc*. **1992**, *114*, 6553.